AIAA -2002-4578

THE MICROWAVE ANISOTROPY PROBE (MAP) MISSION

F. Landis Markley
Aerospace Engineer, Fellow AIAA

James R. O'Donnell, Jr.,
Aerospace Engineer, Member AIAA

Stephen F. Andrews
Aerospace Engineer

David K. Ward,
Aerospace Engineer, Member AIAA

NASA's Goddard Space Flight Center, Greenbelt, MD, 20771, USA

ABSTRACT

The Microwave Anisotropy Probe mission is designed to produce a map of the cosmic microwave background radiation over the entire celestial sphere by executing a fast spin and a slow precession of its spin axis about the Sun line to obtain a highly interconnected set of measurements. The spacecraft attitude is sensed and controlled using an inertial reference unit, two star trackers, a digital sun sensor, twelve coarse sun sensors, three reaction wheel assemblies, and a propulsion system. This paper presents an overview of the design of the attitude control system to carry out this mission and presents some early flight experience.

INTRODUCTION

The Microwave Anisotropy Probe (MAP), the second Medium-Class Explorer (MIDEX) mission, was launched on June 30, 2001 as a follow-on to the Cosmic Background Explorer (COBE), which made precise measurements of the Cosmic Microwave Background (CMB) that is believed to be a remnant of the Big Bang marking the birth of the universe.[1–4] Figure 1 is an equal-area plot in galactic co-ordinates of the anisotropy in the temperature of the CMB as measured by the Differential Microwave Radiometer (DMR) instrument on COBE. The red band along the equator is due to local microwave radiation from our galaxy; it is not related to the CMB. MAP has been designed to measure the CMB anisotropy with sensitivity 50 times that of DMR and angular resolution 30 times finer, specifically 20 microKelvin and 14 arc minutes, respectively, as simulated in Figure 2.[5] These increases in sensitivity and resolution will enable scientists to determine the values of key cosmological parameters and to answer questions about the origin of structure in the early universe and the fate of the universe.[6]

Figure 1: COBE 4-Year CMB Map

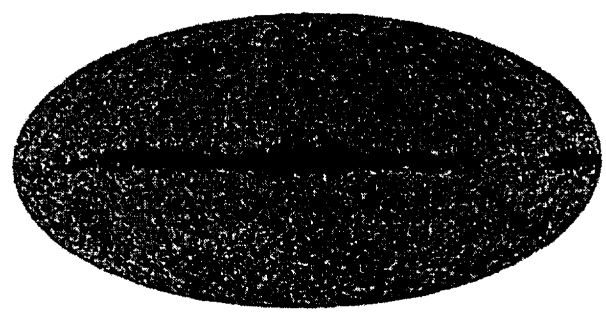

Figure 2: Simulated MAP CMB Map

Since the major error sources in the DMR data arose from COBE's low Earth orbit, MAP was placed in a Lissajous orbit around the Sun-Earth L_2 Lagrange point to minimize magnetic, thermal, and radiation disturbances from the Earth and Sun. MAP attained its Lissajous orbit around L_2 in early October 2001, about 100 days after launch, using a lunar gravity assist following three phasing loops, as shown in Figure 3.[7]

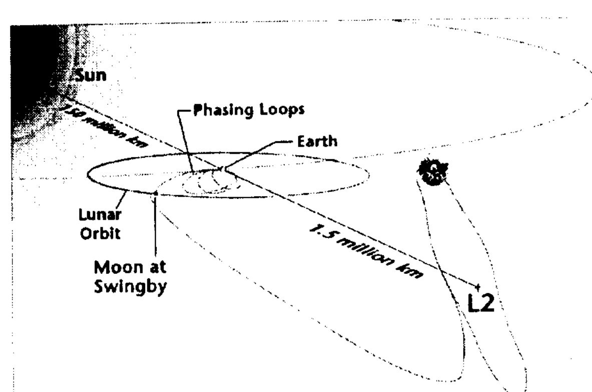

Figure 3: MAP Trajectory to L_2

The MAP instrument includes radiometers at five frequencies, passively cooled to about 90°K, covering two fields of view (FOVs) 141° apart on the celestial sphere. The MAP observatory executes a fast spin at 0.464 rpm and a slower precession of its spin axis at one revolution per hour at a constant angle of 22.5° from the Sun line to obtain a highly interconnected set of measurements over an annulus between 87° and 132° from the Sun. Figure 4 shows the scan pattern covered by one of the two FOVs in one complete spacecraft precession (1 hour), displayed in ecliptic coordinates in which the ecliptic equator runs horizontally across the map. The bold circle shows the path for a single spin (2.2 minutes). As the Earth revolves around the Sun, this annulus of coverage revolves about the ecliptic pole. Thus the entire celestial sphere will be observed once every six months, as shown in Figure 5, or four times in the planned mission life of two years.

This paper give an overview of the Attitude Control System (ACS) that acquires and maintains the spacecraft orbit, controls the spacecraft angular momentum, provides for safety in the event of an anomaly, and implements the spin-scan observing strategy while minimizing thermal and magnetic fluctuations, especially those synchronous with the spin period. More detail can be found in Refs. 8 and 9.

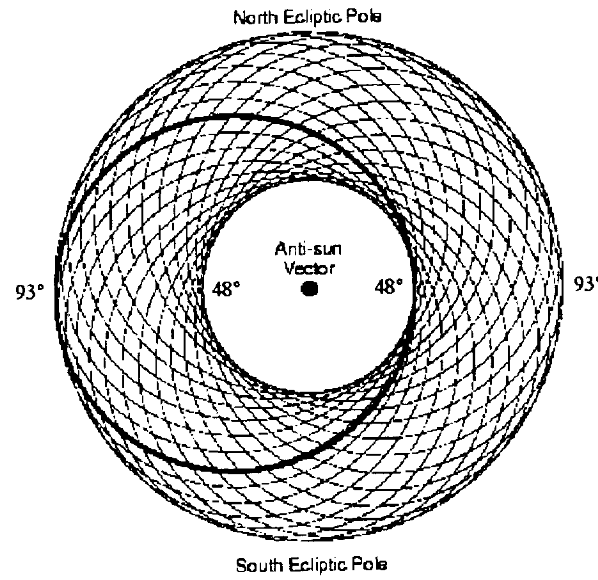

Figure 4: MAP Scan Pattern

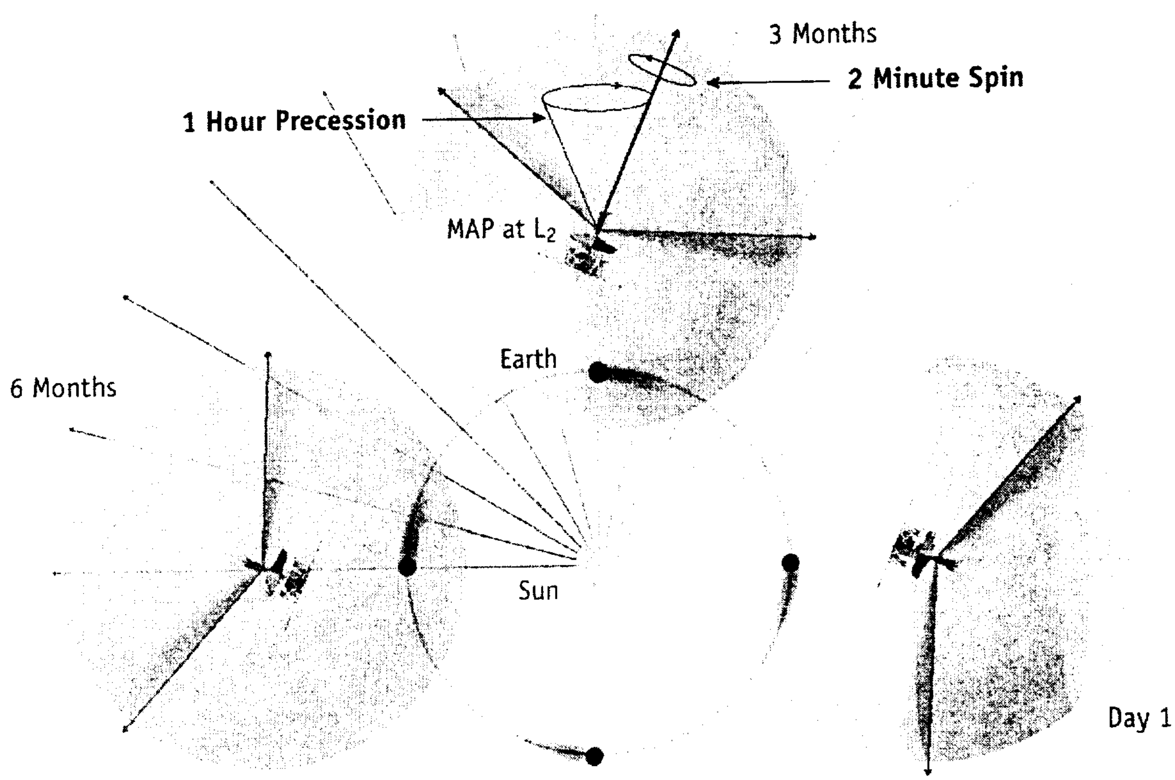

Figure 5: MAP Spin-Scan Concept

ACS OVERVIEW

MAP uses three right-handed, orthonormal co-ordinate systems. The Geocentric Inertial frame (GCI) is an Earth-centered frame with its $\mathbf{x}_I$ axis pointing to the vernal equinox, its $\mathbf{z}_I$ axis pointing to the North Celestial Pole (parallel to the Earth's spin axis), and $\mathbf{y}_I = \mathbf{z}_I \times \mathbf{x}_I$. The Rotating Sun Referenced frame (RSR) is a spacecraft-centered frame in which the $\mathbf{z}_R$ axis points from the MAP spacecraft to the Sun, $\mathbf{x}_R$ is a unit vector in the direction of $\mathbf{z}_R \times \mathbf{z}_I$, and $\mathbf{y}_R = \mathbf{z}_R \times \mathbf{x}_R$. The RSR frame rotates at approximately 1°/day with respect to the GCI frame. The body frame is centered at the spacecraft center of mass with $\mathbf{z}_B$ axis parallel to the spacecraft centerline, directed from the instrument to the solar arrays, $\mathbf{y}_B$ axis normal to the instrument radiator faces, and $\mathbf{x}_B = \mathbf{y}_B \times \mathbf{z}_B$, as shown in Figure 6.

The MAP attitude is sensed by an Inertial Reference Unit (IRU), two Autonomous Star Trackers (ASTs), a Digital Sun Sensor (DSS), and twelve Coarse Sun Sensors (CSSs); it is controlled by three Reaction Wheel Assemblies (RWAs), and a propulsion system.

The IRU comprises two Kearfott Two-Axis Rate Assemblies (TARAs), one with input axes aligned with the $\mathbf{z}_B$ and $\mathbf{x}_B$ axes and the other with input axes aligned with the $\mathbf{z}_B$ and $\mathbf{y}_B$ axes. This gives redundant rate inputs on the $\mathbf{z}_B$ axis; the DSS outputs can be differentiated to provide rates on the other axes in the event of an IRU failure.

The boresights of the two Lockheed-Martin ASTs are in the $\pm\mathbf{y}_B$ directions. Each AST tracks up to 50 stars simultaneously in its 8.8° square FOV, matches them to stars in an internal star catalogue, and computes its attitude as a GCI-referenced quaternion with accuracy of 21 arc-seconds (1σ) around its boresight axis and 2.3 arc-second s (1σ) in the other two axes.

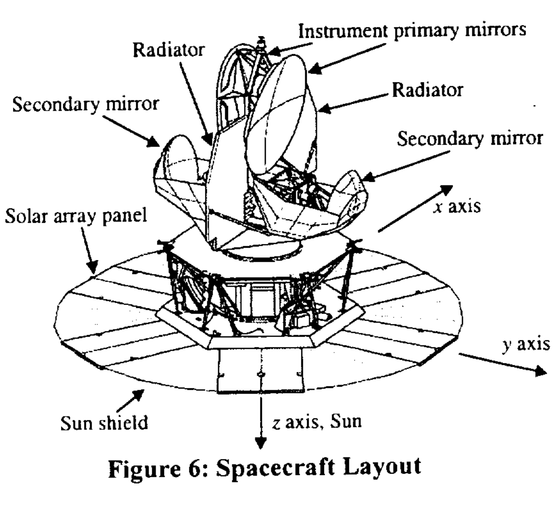

Figure 6: Spacecraft Layout

The Adcole two-axis DSS has two heads, each with 64° square FOV and an accuracy of 1 arc-minute (3σ). The centers of the FOVs of the two heads are in the $\mathbf{x}_B$-$\mathbf{z}_B$ plane at angles of ±29.5° from the $\mathbf{z}_B$-axis. The CSSs are cosine eyes located in pairs looking outward from the edges of the six solar array panels, alternately pointing 36.9° up and 36.9° down from the $\mathbf{x}_B$-$\mathbf{y}_B$ plane.

The RWAs are Ithaco Type E wheels each with a momentum storage capacity of 70 Nms. The available reaction torque of each wheel is 0.35 Nm, but this is limited to 0.215 Nm by the MAP software to satisfy power constraints. The reaction wheel rotation axes are tilted 60° from the $-\mathbf{z}_B$ axis and uniformly distributed 120° apart in azimuth about this axis. The wheels serve the dual function of counterbalancing the body's spin angular momentum to maintain the system momentum (i.e. body plus wheels) near zero while simultaneously applying control torques to provide the desired spacecraft attitude. The wheel axis orientations result in all wheel speeds being biased away from zero while the spin-scan observing motion is being executed, thus avoiding zero-speed crossings that would occur if the wheel spin axes were oriented along the spacecraft body frame co-ordinate axes.

The propulsion system comprises eight monopropellant hydrazine Reaction Engine Modules (REMs) and associated hardware. Each REM generates a maximum thrust of 4.45 N.

More detail on the MAP ACS hardware suite can be found in Ref. 14.

MOMENTUM MANAGEMENT

The choice of an L_2 orbit to minimize magnetic, thermal, and radiation disturbances precludes the use of magnetic sensing or torquing. Thus, the propulsion system provided for orbit maneuvers and stationkeeping is also used to unload accumulated system angular momentum after each orbit adjust. These occur several times in the phasing loops but no more than once every three months at L_2 to minimize interruptions of science observations. The RWAs can store on the order of 70 Nms of angular momentum in non-spinning modes, and a significant fraction of this along the $\mathbf{z}_B$ axis while spinning about this axis. While executing the Observing Mode spin-scan, however, the transverse momentum storage capacity (i.e. in the $\mathbf{x}_B$-$\mathbf{y}_B$ plane) is limited to 3 Nms, the amount that can be cycled among the three RWAs at the fast spin rate without adversely affecting attitude control.

Gravity-gradient, atmospheric drag, and outgassing torques are significant in the phasing loops; but the accumulated angular momentum of less than 1 Nms per orbit is easily stored until removal following orbit maneuvers at apogee or perigee.

Solar radiation pressure torque is the only significant disturbance torque at L_2, and the uniform rotation of the spin axis reduces its average along the $\mathbf{x}_B$ and $\mathbf{y}_B$ axes by more than two orders of magnitude compared to its instantaneous value. The only problematic component would arise from a "pinwheel" torque along the $\mathbf{z}_B$ axis, which might result from an imperfect deployment of the solar array panels. The angular momentum is accumulated in inertial space, so it is clear from Figure 5 that the pinwheel torque at one point in the orbit leads to a transverse angular momentum one-quarter orbit, or 91 days, later. This means that any accumulation of angular momentum from the pinwheel torque of more than about 0.03 Nms per day would require momentum unloading more frequently than desired.

Pre-flight estimates of the pinwheel torque gave angular momentum accumulation ranging from 0.0016 to 0.065 Nms per day, depending on the accuracy of deployment of the solar arrays and the resulting symmetry of the spacecraft.[8] The worst-case estimate would reach the Observing Mode system angular momentum limit of 3 Nms in 46 days, which is highly undesirable. Flight data indicates an angular momentum accumulation of about 0.006 Nms per day, which easily meets the three-month requirement. In fact, since this is less than 0.03 Nms per day, Figure 5 shows that the pinwheel torque will begin to unload the accumulated angular momentum on the next quarter orbit, so no unloading by the REMs is required at all, in principle. The orbit perturbations at L_2 have also been well within requirements, so the current plan is to perform stationkeeping and momentum unloading only once every four months, rather than every three months.

ACS OPERATIONAL MODES

MAP has six ACS modes. The Observing, Inertial, Delta V, Delta H, and Sun Acquisition modes are implemented in the main spacecraft (Mongoose V) processor, while the Safehold Mode resides in the Attitude Control Electronics Remote Services Node (ACE RSN). Figure 7 shows the modes and the transitions among them. Anomalous behavior can result in autonomous transitions from any other mode to Sun Acquisition Mode or Safehold Mode, even though these transitions are not shown explicitly. The ACS modes are discussed below, including the sensors, actuators, and control algorithms used.

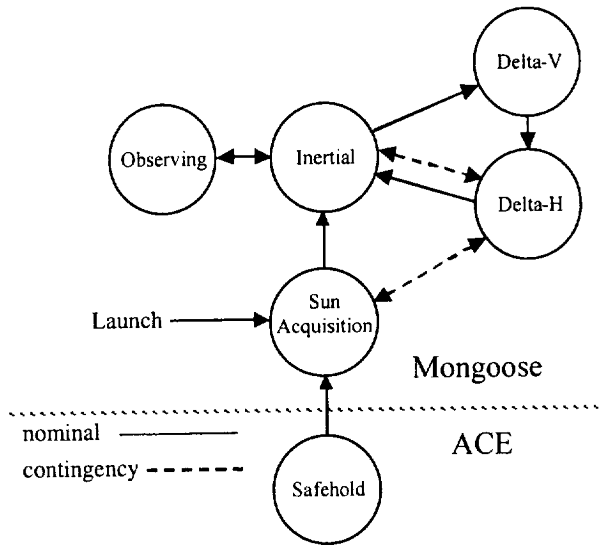

Figure 7: ACS Mode Transitions

Observing Mode

Observing Mode is used for science operations to maintain the 22.5°±0.25° angle between the spin axis and Sun line and to implement the observing strategy shown in Figures 4 and 5. This is accomplished by specifying the Observing Mode attitude of the MAP spacecraft with respect to the RSR co-ordinate frame by the set of 3-1-3 Euler angles[10, 11]

$$\phi_c = \phi_0 + \int_{t_0}^{t} \dot{\phi}_c dt, \tag{1a}$$

$$\theta_c = 22.5° = 0.3927 \text{ rad}, \tag{1b}$$

$$\psi_c = \psi_0 + \int_{t_0}^{t} \dot{\psi}_c dt, \tag{1c}$$

where $\dot{\phi}_c = -1 \text{ rev/hour} = -0.001745 \text{ rad/sec}$ and $\dot{\psi}_c = 0.464 \text{ rpm} = 0.04859 \text{ rad/sec}$ are the desired spin-scan rates, and initial conditions determine ϕ_0 and ψ_0. A commanded RSR-to-body quaternion and angular rate vector are computed from these Euler angles and rates by the standard equations.[10, 11] An estimated RSR-to-body quaternion and angular rate vector are computed using IRU, AST, and DSS measurements in a Kalman Filter combined with a GCI-to-RSR quaternion computed onboard from ephemeris models. The desired control torque is computed by a proportional-derivative (PD) controller using RSR-to body quaternion and rate errors.[15, 16] A feedforward term including the commanded angular acceleration and a gyroscopic term is added to reduce hangoff. The commanded torque is distributed to the RWAs using a torque distribution matrix defined by the orientation of the RWAs in the body co-ordinate system. Normal exit from Observing Mode is by command only.

Inertial Mode

As shown in Figure 7, Inertial Mode acts as a staging mode between the other operations of the spacecraft. This is an RWA- and IRU-based mode similar to Observing Mode, using the same Kalman Filter, but differs in that the commanded rates are zero and the feedforward terms are absent. Inertial Mode can either hold the spacecraft in an inertially fixed orientation or slew the spacecraft to a sequence of GCI-to-body quaternions from a Command Quaternion Table (CQT) uploaded from the ground. A slew is executed if the desired orientation is not close to the current spacecraft orientation. Normal exits from Inertial Mode are by command only.

Delta V Mode

Delta V Mode, which uses the REMs to adjust the orbit in either the initial phasing loops or for L_2 stationkeeping, is only entered from Inertial Mode by a command sequence specifying burn duration, direction and start time. The desired attitude (in terms of a single quaternion or a CQT) and thrusters to be used can be configured either via command or by table load. The spacecraft remains in Inertial Mode to slew from the initial orientation to the desired attitude for the start of the delta V, and transitions to Delta V Mode at the start time of the requested burn. The only sensors used in Delta V Mode are the IRU and RWA tachometers. This mode uses a PD controller to hold the spacecraft to a commanded quaternion attitude while executing the Delta V burn. The output of the controller is transformed into thruster firing commands using a pulse width modulator with a minimum pulse width of 0.04 sec. The desired attitude is held by off-pulsing the primary set of thrusters and on-pulsing the others. Normal exit is autonomously to Delta H Mode

Delta H Mode

Delta H Mode uses the REMs to unload spacecraft system angular momentum, which is computed using the RWA tachometers and IRU. It is used primarily upon exit from Delta V Mode; but can be commanded from Inertial or Sun Acquisition Mode if necessary, although this is not anticipated. The same pulse width modulator is used for Delta H as for Delta V, with the exception that all thrusters are operated in an on-pulsing manner for Delta H. If entry was from Delta V or Inertial Mode, the ACS autonomously transitions to Inertial Mode after the momentum has been reduced to less than 0.3 Nms. If Delta H Mode was entered from Sun Acquisition Mode, as discussed below, the autonomous exit upon completion of the momentum unloading is back to Sun Acquisition Mode.

Sun Acquisition Mode

Sun Acquisition Mode uses the CSS, IRU, and RWAs to acquire and maintain a thermally safe power-positive orientation, with the spacecraft $\mathbf{z}_B$ axis within 25° of the Sun. Upon separation from the launch vehicle, MAP is in Sun Acquisition Mode, which must slew the spacecraft from any initial angle and any initial body momentum less than [13, 13, 55] Nms to a power-positive orientation within 40 minutes. If the body momentum exceeds the amount that can be handled by Sun Acquisition Mode, Delta H Mode is commanded to reduce the momentum to an acceptable level, after which the spacecraft returns to Sun Acquisition Mode. Transition to Inertial Mode can be commanded after the attitude has been initialized. Transition to the Mongoose control modes from the ACE Safehold Mode is through Sun Acquisition Mode.

Safehold Mode

Safehold Mode is implemented in the ACE, so it can be entered autonomously in the event of a Mongoose anomaly. It has two configurations, which differ by the rate information used. The first, Safehold/IRU, is a copy of the Sun Acquisition Mode in the Mongoose. The second, Safehold/CSS, is a minimum-hardware mode using only the RWAs and CSSs, with rate errors being computed by numerically differentiating the position error signals. Because it lacks body z rate information from the gyros, Safehold/CSS can tolerate less system momentum than can Sun Acquisition or Safehold/IRU Mode. Since the CSSs are insensitive to rotations about the Sun line, anti-runaway compensation is applied to prevent the wheels from uncontrolled spinning about the satellite's z-axis. This is accomplished by applying equal damping torques to the three wheels if the sum of their speeds exceeds a pre-set value, thereby suppressing z-axis rotation without applying a net torque in the x-y plane. Exit from either Safehold Mode is by ground command only.

FLIGHT SOFTWARE

By the preliminary design stage for the MIDEX program, tools existed that would make design, analysis and development an integrated process, allowing a reduction in manpower and a reduction in development time, consistent with the philosophy of the MIDEX program. There was also an interest in reusing software and developing reusable model/software libraries for quicker mission designs in the future. The MatrixX integrated analysis and design toolset from Integrated Systems, Inc. was selected because it possessed the desired capabilities. The MatrixX components used for MAP include a linear analysis tool (XMath), a graphical environment for developing and executing nonlinear simulations (SystemBuild), an automatic code generation product (AutoCode), and a documentation generation product (DocumentIt).[17-19]

Automatic Code Generation

The decision to use automatically-generated code was an attempt to address some of the lessons learned from previous in-house spacecraft developments at Goddard, such as the Rossi X-Ray Timing Explorer (RXTE) and Tropical Rainfall Measuring Mission (TRMM). Following the RXTE and TRMM ACS developments, a need was seen to limit the manual interfaces required to design and develop an ACS subsystem. The previous design system was characterized by a large duplication of effort, with three separate teams—the analysts, the flight software developers, and the developers of the hybrid dynamic simulator (HDS) used to test the flight software—designing the same system independently.

An overview of the previous design process, depicted in Figure 8, shows that the analysis, simulation, code, and test efforts were developed independently, rather than branching from a single design point. This process relied on written documentation to describe changes in the design that needed to be reflected in all three systems. One person was dedicated to the development of the high fidelity simulation (HiFi), which was not useful in the linear analysis of the system, and another person was a dedicated documentation engineer, needed to keep the flight software and test simulation teams informed of changes. This process was prone to manual implementation errors and misunderstandings, which resulted in the FSW team not always initially implementing the algorithms as the design team had envisioned them. Additionally, the Hybrid Dynamic Simulator (HDS), designed to test the flight software, was designed by a separate team and was unable to benefit from any efficiencies of co-development.

The MatrixX software was used to create a single design point in the HiFi simulation that every team member could use, rather than needing one HiFi and several low fidelity simulations. The same HiFi could be used for the linear stability analysis and, using other add-ons in the MatrixX toolkit, could be the basis of automatic code and documentation generation. This eliminated a significant manual documentation and translation effort and had the significant additional benefit of ensuring that all members of the ACS design team were working from the same single design point. It also reduced the risk of errors associated with manual translation. The process used for the MAP software development is shown in Figure 9.

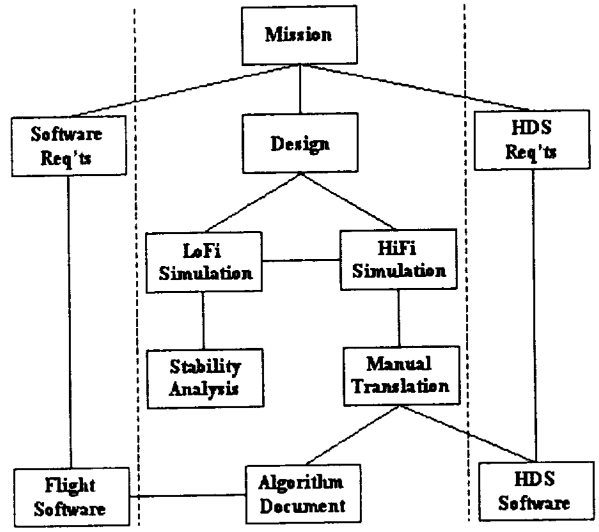

Figure 8: Previous Development Process

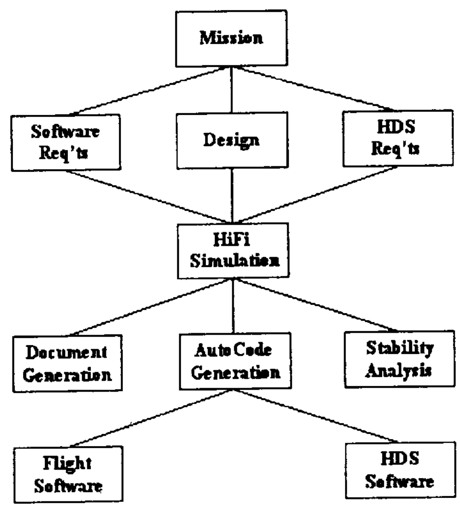

Figure 9: Integrated Development Process

The MAP software development was based on HiFi, as shown in Figure 9, but the HDS software was not AutoCoded. This minimized the risk of an error going undetected by being replicated in both places. AutoCode was used for the control law algorithms and system momentum calculations in the Mongoose V flight software only, and not in the ACE software. This limited risk by not automatically generating code for any flight software component that required a direct interface to ground commands or to the spacecraft sensors and actuators. Further, because the control laws had a high algorithm-to-code ratio and a clearly defined interface to the rest of the system, they provided a good test of the code-generation method. A final benefit to using AutoCode primarily on the spacecraft control laws is that these are good candidates for reuse on future missions.

Automation of Software Testing

RXTE and TRMM flight software test procedures were developed on the ground system. The initial conditions for these tests were then given to an ACS analyst to replicate the initial conditions in HiFi, which were used to define the expected test results. The flight software test procedures were executed in the flight software lab. The results were plotted using the test author's favorite plotting package, which was usually different from any of the other tester's favorite plotting package. The resulting plots from the HiFi and the flight software test execution were then held side to side and visually compared. The plethora of variables that needed to be consistent between the HiFi, HDS, and flight software were maintained in a spreadsheet and manually entered into the HiFi, HDS, and flight software. Figure 10 shows this process. As denoted by the gray shaded arrows, there were many manual steps in this process that were prone to errors.

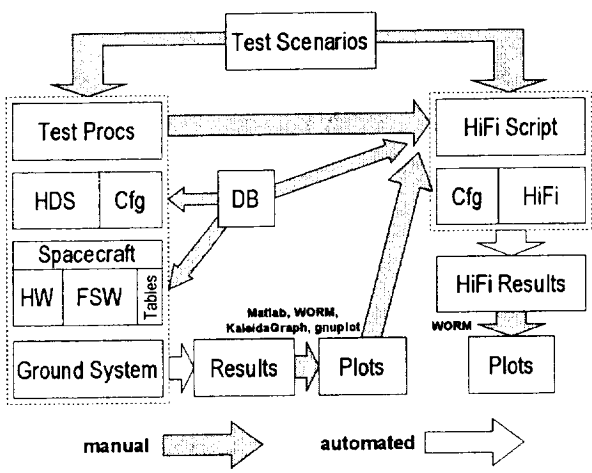

Figure 10: Manual Flight Software Test Process

The RXTE/TRMM process encountered pitfalls in each of these manual steps, namely replicating the initial conditions, plotting of the results, and maintaining consistency between all of the variables. Especially in the infancy of these flight software test programs, it was not unusual to go through several iterations of a particular test, trying to match the initial conditions and variables. Inconsistencies would be discovered in the plot results review; for example, that the Kalman filter was not enabled in the flight software test but was enabled in the HiFi version of the test, creating different results. Sometimes the inconsistencies were more subtle, such as a number swap of one of the digits of a variable. Time-consuming iterations were also made in the plotting process, since consistency in scaling and units between the flight software and HiFi plots is extremely important. Many times, the flight software plots would have to be recreated in order to scale the plots with enough detail to verify the results with HiFi or to change the units to facilitate comparison.

Finally, the separate nature of the flight software testing and HiFi paths slowed the verification process. The HiFi runs could only be created by a member of the ACS analysis team familiar with the HiFi, and could only be executed with any confidence after the flight software test results were reviewed. The limited number of analysts, as well as the fact that the analyst would need multiple interactions with the tester for each test, frequently created test verification bottlenecks.

On MAP, many of the manual processes were automated, streamlining the testing process.[20] Figure 11 illustrates the flight software test flow that MAP followed, highlighting the areas that were automated. In contrast with RXTE/TRMM, MAP had tools for dissecting a flight software test procedure and automatically producing a HiFi script that replicated the flight software test procedure flow. In addition, MAP had a centralized database that defined and linked all of the variables used in HiFi, HDS, and the flight software. With the press of a button, the database generated the source files for each of these systems that guaranteed consistency. Finally, the plotting process was streamlined since the MAP tools defined a standard set of plots that were used to present the flight software, HiFi, and HDS test results on one plot.

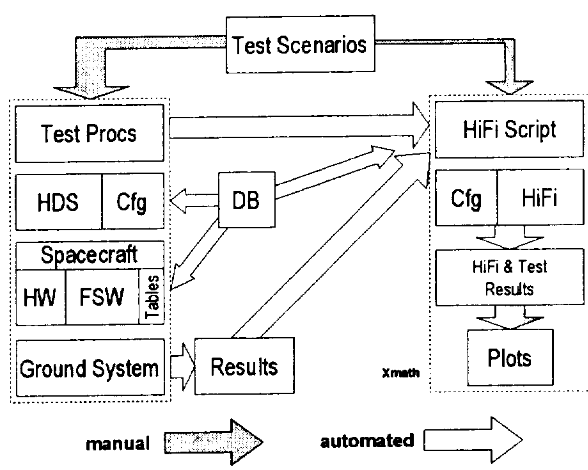

Figure 11: Automated Flight Software Test Process

One of the keys to the success of the MAP flight software testing effort was the parameter database used for configuration management of virtually all the variables, control gains, failure detection and correction (FDC) parameters, and other parameters used by the MAP ACS. As shown in Figure 11, the database fed into all of the ACS elements. As each parameter was placed in the MAP database, it was assigned to an appropriate subsystem engineer to populate the database with the correct information and verify it.

Upon release each new version of flight software for either the spacecraft main processor or attitude control electronics, a corresponding release from the MAP database was created. Output templates from the database were created as header files for the flight software; additionally, script files for initializing the HDS and HiFi were generated at the same time. In this way, a consistent set of parameters across each test system component was assured for flight software tests and HiFi verification simulations.

The MatrixX integrated toolkit, its Xmath command environment, and its SystemBuild simulation component lend themselves especially well to this automation process. The MathScript scripting language, based on Xmath, acts as the glue that holds the simulation and testing process together. It was used extensively with the MAP HiFi to set up simulations and to perform many data analysis functions. MathScript allows flight software and HiFi simulation to be analyzed, interfaces with MatrixX's SystemBuild simulation environment to allow simulations to be created and run, and provides the mechanism for creating comparison plots between flight software and HiFi simulation verification data.

MathScript is a complete scripting language for data processing, particularly matrix processing, and provides all of the functions necessary for interfacing numerical data and the HiFi simulation, but it lacks extensive string processing capability. However, MathScript's ability to interface with the native operating system makes it possible to add the string processing functions needed to process Systems Test and Operations Language (STOL) procedures, Record Definition Language statements (RDLs), and the sequentially printed data output files from the MAP ground system, which are mixed numeric and text. Test data can be read in and processed using string processing extensions programmed in Perl. Using SystemBuild Access, an extension to Xmath that allows it to access and control SystemBuild simulations, MathScript functions can create and run HiFi simulations to perform data analysis and test verification.

It should be noted that while the MatrixX integrated toolkit lends itself particularly well to the design of automated test tools, such tools could be designed in other settings. The key ingredient is a scripting language around which the rest of the system can be built. The Matlab/Simulink environment, using Matlab's m-file scripting, could also be used. Even a dedicated simulation such as one written in a language such as FORTRAN or C can be used with these automated test techniques.

FLIGHT EXPERIENCE

The Delta launch vehicle placed the MAP spacecraft on a very accurate trajectory with body angular momentum of only 6.2 Nms at separation, well within the capability of the Sun Acquisition Mode, which acquired the Sun within 15 minutes. Maximum pointing errors during the nine Delta V maneuvers performed in the first three months of the mission were smaller than predicted (3.7° vs. 5.5°), and imparted velocity increments were accurate to 1%. Less than 15 kg of hydrazine propulsion fuel was expended to get to L_2, about half the amount budgeted for this phase of the mission. The 57 kg of fuel remaining for stationkeeping and momentum unloading at L_2 will easily support a four-year extended mission.

Stray light in the ASTs caused some problems during the phasing loops. Both ASTs lost track when the Moon was within a degree or so of the FOV, but only for a few seconds in a spin cycle, and only for three spin cycles in any precession cycle. No more than 13 AST readings were lost in a precession cycle. There is no Moon, Earth, or Sun interference at L_2, and the ASTs have been routinely tracking 15 to 40 stars in the absence of interference. Attitude knowledge has been better than 20 arc seconds per axis, easily meeting the three-axis root-sum-square requirement of 78 arc seconds. The Sun angle has been maintained between 22.44° and 22.54° in Observing Mode, as illustrated by the perfect circle traced by the Sun vector over several hours in Figure 12.

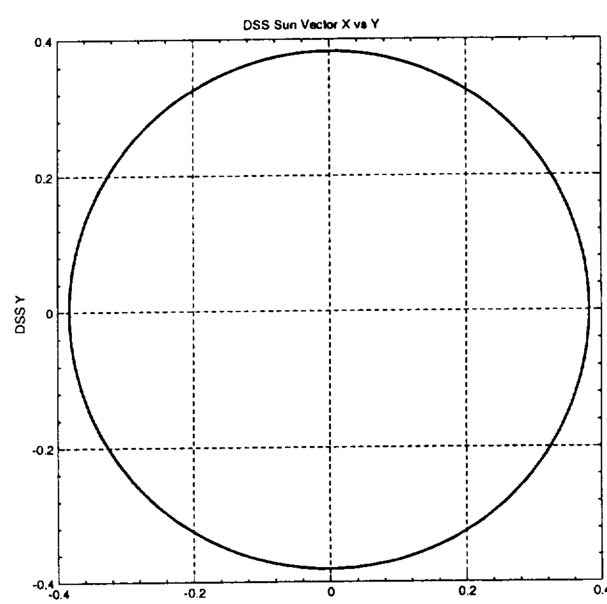

Figure 12: DSS Measurements in Observing Mode

Initially, the precession rate $\dot{\phi}$ in Observing Mode did not meet its 5% accuracy requirement, showing a 7% variation at the spin period. This was attributed to an inaccurate value of system momentum in the gyroscopic feedforward loop arising from a scale factor error in the RWA tachometer signals. Evidence for this was that the magnitude of the system momentum, which should be constant, had a 0.4 Nms oscillation at spin period and increased during spin-up by 1.0 Nms. Comparing a high-fidelity simulation with flight data determined that the oscillation and spin-up offset could be removed by a small change in the tachometer scale factors by about 2.5% for RWA1 and about 4% for RWA2 and RWA3. After loading these new scale factors, the variation of the precession rate was dramatically reduced, as were the spin-period oscillation and the spin-up offset in the computed system momentum magnitude shown in Figure 13.

Charged particle flux from extreme solar activity on November 5, 2001 caused a power-on reset of the Mongoose processor. The ACS transitioned autonomously to Safehold Mode in the ACE, which functioned exactly as designed to keep MAP safe. The transition to Safehold Mode was discovered by operations staff at the next telemetry pass about 12 hours later, and recovery to Observing Mode was accomplished within three hours of this discovery.

CONCLUSIONS

The Microwave Anisotropy Probe attitude control system was designed and developed more efficiently than those of previous missions. Flight software development was facilitated by use of integrated analysis and design tools to increase the flight software team's communication and integrate their work more tightly. Team members abandoned the specialization found on previous programs; analysts; flight software developers, systems engineers and testers shared a common design point. Standardizing interfaces and test procedures and developing new data analysis tools removed many of the testing bottlenecks encountered in previous programs, so that a number of rounds of regression testing to accommodate late software changes and additions could be performed in a very timely, efficient, and thorough manner.

The attitude control system described in this paper and developed using these tools has successfully met the demanding requirements of the Microwave Anisotropy Probe mission. These include the need to function robustly far from the Earth where no magnetic field is useful for sensing or actuation, and with infrequent telemetry passes. The processor upset on November 5, 2001 illustrated the importance of having a safemode control capability that is independent of the primary control hardware and software.

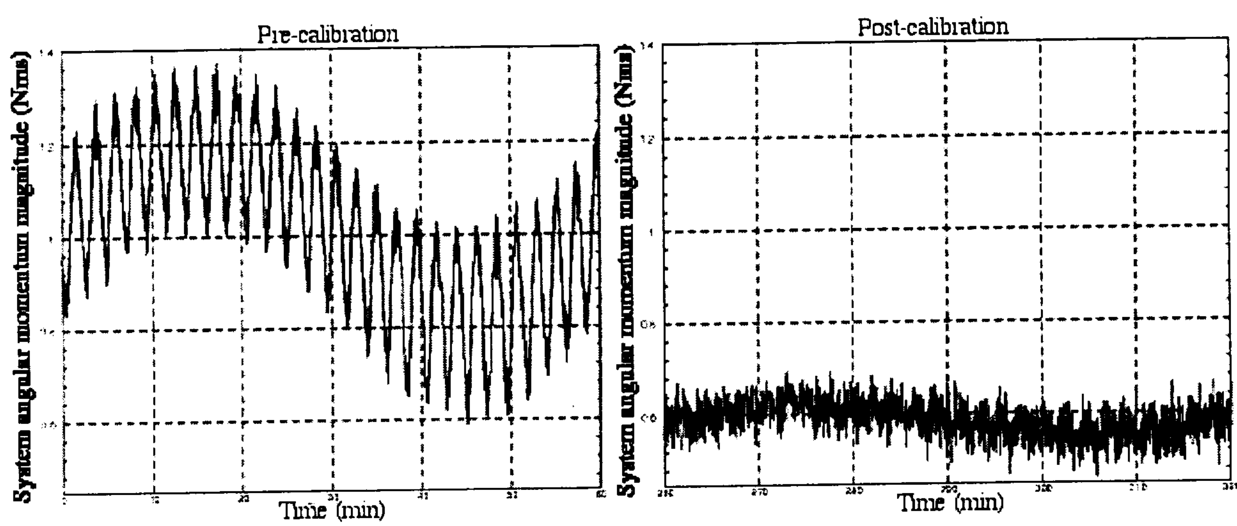

Figure 13: Pre- and Post-Calibration System Angular Momentum Magnitude

REFERENCES

1. Boggess, N. W., *et al.*, "The *COBE* Mission: Its Design and Performance Two Years After Launch," *Astrophysical Journal*, Vol. 397, No.2, pp. 420-429, 1992

2. Gulkis, S., Lubin, P. M., Meyer, S. S., and Silverberg, R. F., "The Cosmic Background Explorer," *Scientific American*, Vol. 262, No. 1, pp. 132-139, 1990

3. Smoot, G. F., *et al.*, "Structure in the *COBE* Differential Microwave Radiometer First-Year Maps," *Astrophysical Journal Letters*, Vol. 396, pp. L1-L5, 1992

4. Bennett, C.L., *et al.*, "Four-Year *COBE* DMR Cosmic Microwave Background Observations: Maps and Basic Results," *Astrophysical Journal Letters*, Vol. 464, pp. L1-L4, 1996.

5. Bennett, C. L., Hinshaw, G. F., and Page L., "A Cosmic Cartographer," *Scientific American*, Vol. 284, No. 1, pp. 44-45, 2001 (see also http://map.gsfc.nasa.gov)

6. Hu, W., Sugiyama, N., and Silk, J., "The Physics of Microwave Background Anisotropies," *Nature*, Vol. 386, No. 6620, pp. 37-43, 1997 (see also http://background.uchicago.edu)

7. Richon, K. V., and Mathews, M. W., "An Overview of the Microwave Anisotropy Probe (MAP) Trajectory Design," *Astrodynamics 1997*, Volume 97, *Advances in the Astronautical Sciences*, edited by F. R. Hoots, B. Kaufman, P. J. Cefola, and D. B. Spencer, San Diego, CA, Univelt, Inc., pp. 1979-1998, 1998

8. Andrews, S. F., Campbell, C. E., Ericsson-Jackson, A. J., Markley, F. L., and O'Donnell, J. R., "MAP Attitude Control System Design and Analysis," *Flight Mechanics Symposium 1997*, NASA CP-3345, Greenbelt, MD, pp. 445-456, 1997

9. Ericsson-Jackson, A. J., Andrews, S. F., O'Donnell, J. R., Jr., and Markley, F. L., "MAP Stability, Design and Analysis," *Spaceflight Dynamics 1998*, Volume 100, *Advances in the Astronautical Sciences*, edited by Thomas H. Stengle, San Diego, CA, Univelt, Inc., pp. 955-969, 1998

10. Wertz, J. R., ed., *Spacecraft Attitude Determination and Control*, Dordrecht, Holland, D. Reidel, 1978

11. Shuster, M. D., "A Survey of Attitude Representations," *Journal of the Astronautical Sciences*, Vol. 41, No. 4, pp. 439-517, 1993

12. Lefferts, E. J., Markley, F. L., and Shuster, M. D., "Kalman Filtering for Spacecraft Attitude Estimation," *Journal of Guidance, Control, and Dynamics*, Vol. 5, No. 5, pp. 417-429, 1982

13. Murrell, J. W., "Precision Attitude Determination for Multimission Spacecraft," *1978 AIAA Guidance and Control Conference*, AIAA Paper 78-1248, Palo Alto, CA, pp. 70-87, 1978

14. Ward, Davis K., and Davis, Gary T., "The Microwave Anisotropy Probe Guidance, Navigation, and Control Hardware Suite," *2002 AIAA Guidance, Navigation and Control Conference*, AIAA Paper 2002-4579, Monterey, CA, 2002

15. Wie, B., and Barba, P. M., "Quaternion Feedback for Spacecraft Large Angle Maneuvers," *Journal of Guidance, Control, and Dynamics*, Vol. 8, No. 3, pp. 360-365, 1985

16. Andrews, S. F. , and O'Donnell, J. R. , Jr.," MAP Attitude Control System Design and Flight Performance," *2002 AIAA Guidance, Navigation and Control Conference*, AIAA Paper 2002-4580, Monterey, CA, 2002

17. McComas, David C., O'Donnell, James R., Jr., and Andrews, Stephen F., "Using Automatic Code Generation in the Attitude Control Flight Software Engineering Process", *23rd Software Engineering Workshop*, NASA Goddard Space Flight Center, Greenbelt, MD, 1998.

18. Ward, David K., Andrews, Stephen F., McComas, David C., and O'Donnell, James R., Jr., "Use of the MatrixX Integrated Toolkit on the Microwave Anisotropy Probe Attitude Control System," *21st AAS Guidance and Control Conference*, Breckenridge, CO, 1999.

19. O'Donnell, James R., Jr., Andrews, Stephen F., David C. McComas, and Ward, David K., "Development and Testing of Automatically-Generated Flight Software for the MAP Spacecraft," *14th International Symposium on Space Flight Dynamics*, Iguassu Falls, Brazil, 1999.

20. O'Donnell, James R., Jr., Morgenstern, Wendy M., and Bartholomew, Maureen O., "Using Automation to Improve the Flight Software Testing Process," *2001 Flight Mechanics Symposium*, NASA/CP-2001-2099865, Greenbelt, MD, pp. 295-309, 2001

GSFC STI PUBLIC DISCLOSURE EXPORT CONTROL CHECKLIST

The Export Control Office requests your assistance in assuring that your proposed disclosure of NASA scientific and technical information (STI) complies with the Export Administration Regulations (EAR, 15 CFR 730-774) and the International Traffic in Arms Regulations (ITAR, 22 CFR 120-130). The NASA Export Control Program requires that every domestic and international presentation/publication of GSFC STI be reviewed through the GSFC Export Control Office in accordance with the NASA Form 1676, NASA Scientific and Technical Documents Availability Authorization (DAA) process. Release of NASA information into a public forum may provide countries with interests adverse to the United States with access to NASA technology. Failure to comply with the ITAR regulations and/or the Commerce Department regulations may subject you to fines of up to $1 million and/or up to 10 years imprisonment per violation. Completion of this checklist should minimize delays in approving most requests for presentation/publication of NASA STI.

Generally, the export of information pertaining to the design, development, production, manufacture, assembly, operation, repair, testing, maintenance or modification of defense articles, i.e., space flight hardware, ground tracking systems, launch vehicles to include sounding rockets and meteorological rockets, radiation hardened hardware and associated hardware and engineering units for these items are controlled by the State Department under the ITAR. A complete listing of items covered by the ITAR can be accessed at http://gsfc-bluenun.gsfc.nasa.gov/export/regsitar.htm. The export of information with respect to ground based sensors, detectors, high-speed computers, and national security and missile technology items are controlled by the U.S. Commerce Department under the EAR. If the information intended for release falls within the above categories but otherwise fits into one or more of the following exemptions, the information may be released.

EXEMPTION I
If your information is already in the public domain **in its entirety** through a non-NASA medium and/or through NASA release previously approved by the Export Control Office, the information is exempt from further review. If the information falls into this category, you may attest that you are using this exemption by signing below.

4/20/02

Signature Date

EXEMPTION II
If your information pertains exclusively to the release of scientific data, i.e., data pertaining to studies of clouds, soil, vegetation, oceans, and planets, without the disclosure of information pertaining to articles controlled by the ITAR or EAR, such as flight instruments, high speed computers, or launch vehicles, the information is exempt from further review. If the information falls into this category, you may attest that you are using this exemption by signing below.

Signature Date

EXEMPTION III

If your information falls into the areas of concern as referenced above, but is offered at a general purpose or high level, i.e. poster briefs and overviews, where no specific information pertaining to ITAR or EAR controlled items is offered, the information is exempt from further review. If the information falls into this category, you may attest that you are using this exemption by signing below.

______________________ ______________

Signature Date

EXEMPTION IV

If your information is not satisfied by the three exemptions stated above, the information may be released using exemption 125.4(b)(13) of the ITAR. Use of this exemption is afforded only to agencies of the Federal Government and allows the release of ITAR controlled information into the public domain. The GSFC Export Control Office has determined that use of this exemption will be allowed only after receiving assurance that such release is a responsible action. The following internal guideline has been established regarding use of this authority: That the information does not offer specific insight into the design, development, production, or manufacture of an identified ITAR controlled item (reference paragraph 2, above) in sufficient detail (by itself or in conjunction with other publications) to allow potential adversaries to replicate the item or exploit or defeat controlled U.S. technologies. All signatures of approval on NASA Form 1676 expressly indicate concurrence with the responsible use of Exemption IV when Exemption IV has been cited by the author. If you determine that you have met this criteria, you may attest your determination by signing below, and the GSFC Export Control Office will offer favorable consideration toward approving your presentation/publication request under this special exemption.

______________________ ______________

Signature Date

If you do not satisfy the above exemptions, please contact the GSFC Export Control Office for further clarification on the releasability of your information under the ITAR or EAR.